Appl Microbiol Biotechnol (2014) 98:1691–1701
DOI 10.1007/s00253-013-5043-2

Heterologous expression, characterization and evaluation of the matrix protein from Newcastle disease virus as a target for antiviral therapies

Nida Iram · Muhammad Salahuddin Shah · Fouzia Ismat · Mudasser Habib · Mazhar Iqbal · S. Samar Hasnain · Moazur Rahman

Received: 3 April 2013 / Revised: 4 June 2013 / Accepted: 7 June 2013 / Published online: 25 June 2013

Abstract Newcastle disease virus (NDV) is an infectious agent of a large variety of birds, including chicken, which poses a real threat to the agriculture industry. Matrix (M) proteins of NDV and many other viruses perform critical functions during viral assembly and budding from the host cell. M-proteins are well conserved and therefore are potential targets for antiviral therapies. To validate this, we expressed the NDV M-protein in its native form in *Saccharomyces cerevisiae* and in inclusion bodies in *Escherichia coli*. Proper refolding of the recombinant protein produced in *E. coli* was verified using circular dichroism and infrared spectroscopies and electron microscopy. Immunization of chickens with the NDV M-protein elicited significant serum antibody titers. However, the antibodies conferred little protection against the ND following lethal viral challenges. We conclude that the M-protein is not exposed on the surface of the host cell or the virus at any stage during its life cycle. We discuss how the conserved M-protein can further be exploited as an antiviral drug target.

Keywords Matrix protein · Recombinant protein · Newcastle disease virus · Virus assembly · Virus budding · Refolding · Immunogenicity

N. Iram · M. S. Shah · F. Ismat · M. Iqbal · M. Rahman (✉)
Drug Discovery and Structural Biology group, Health Biotechnology Division, National Institute for Biotechnology and Genetic Engineering (NIBGE), Faisalabad, Pakistan
e-mail: moazur@yahoo.com

M. Rahman
e-mail: moaz@nibge.org

M. S. Shah · M. Habib
Vaccine Development group, Animal Sciences Division, NIAB, Faisalabad, Pakistan

S. S. Hasnain · M. Rahman
Molecular Biophysics group, Faculty of Life Sciences, University of Liverpool, Liverpool, UK

N. Iram · M. Rahman
Pakistan Institute of Engineering and Applied Sciences, P.O. Nilore, Islamabad, Pakistan

Introduction

Newcastle disease virus (NDV) is member of the avian *Paramyxoviridae* (order of the *Mononegavirals*). An infectious agent of chickens, it represents a major threat to the poultry industry (Yusoff and Tan 2001). Viral replication, transcription, translation, and protein processing occur in the cytoplasm of the host cell, while virus particles are assembled in plasma membrane by budding (Peeples et al. 1992; Zanetti et al. 2003). NDV contains a nonsegmented, negative-sense RNA genome encoding for six major structural proteins (from 5′ to 3′): a large RNA-directed RNA-polymerase, a hemagglutinin-neuraminidase (HN), a fusion protein (F), a matrix protein (M), a phosphoprotein (P), and a nucleoprotein (NP).

NDV is enveloped by a lipid bilayer derived from the host-cell membrane with membrane-embedded spikes consisting of glycosylated HN and F-proteins projecting from the surface. The envelope encapsulates the M-protein and the RNA genome, together constituting the viral transcriptase complex (Yusoff and Tan 2001). The M-protein is the smallest nonglycosylated structural protein of NDV, approximately 40 kDa in size and is conserved among NDV strains (Chambers et al. 1986; Yusoff and Tan 2001; Seal et al. 2000). Mutations in the M-protein decrease the incorporation of the glycoprotein fusion into viral particles and ultimately

decreases their virulence (Peeples and Bratt 1984). The M-protein plays key roles in virus assembly and budding via its interaction with the N-terminal cytoplasmic tail of glycoproteins HN and F and NPs subunits, as well as with various elements of host (Panshin et al. 1997; Pantua et al. 2006; Adu-Gyamfi et al. 2013; Yusoff and Tan 2001). M-proteins from various members of the order *Mononegavirales* have been shown to oligomerize into a matrix layer under the lipid membrane during process of virus assembly and budding (Zhang et al. 2012; Harrison et al. 2010; Hoenen et al. 2010). In Ebola viruses, the hydrophobic C-domain of the M-protein facilitates membrane localization, protein oligomerization, and virus particle egress (Adu-Gyamfi et al. 2013).

An electron microscopy reconstruction of the M-layer and a crystal structure of the NDV M-protein were recently reported (Battisti et al. 2012). The potential use of the M-protein as an antiviral target, however, has not yet been established. Considering the importance of the M-protein in the virus life cycle, we therefore expressed the NDV M-protein in yeast and *Escherichia coli*. The protein is expressed at high amounts in inclusion bodies in *E. coli* and refolded to its native form in the presence of detergent. The effect of immunization with the M-protein against NDV lethality was assessed in chickens.

Material and methods

Propagation of Newcastle disease virus

For propagation of NDV, lyophilized vaccine against NDV from Sindh Poultry Vaccine Centre Karachi, solubilized in 2 mL of normal saline (0.89 % NaCl) or field isolates harvested by trituration and centrifugation from infected provetriculi were injected (100-μL volume) into allantoic cavity of 9th-day-old embryonated chicken eggs. After 48 h of inoculation the allantoic fluid was collected as described (Grimes 2002) with slight modifications. Presence and titer of virus was determined by hemagglutination test (Hierholz et al. 1969).

Extraction of viral RNA and cDNA synthesis

Viral RNA was extracted by Guanidinium thiocyanate-phenol-chloroform (TRI reagent®) exaction method (Chomczynski and Sacchi 1987). For this, 1 mL of TRI reagent® (MRC-USA) was added to 0.3 mL of allantoic fluid and mixed well to get homogenous suspension. Following this, 0.2 mL chloroform was added and aqueous phase containing RNA was collected. RNA was precipitated with the addition of 0.5 mL of 100 % isopropanol and pelleted by centrifugation at 16,000×*g*. RNA pellet was then washed with 1 mL of 75 % ethanol, vacuum dried, and resupended in RNase-free water.

cDNA was synthesized with first strand cDNA synthesis kit (Fermentas cat# K1612) using random hexamers primers as per recommendations of manufacturer.

Construction of expression vectors

Nucleotide sequences of NDV matrix gene of a number of isolates from South Asian region were retrieved from NCBI GenBank, and primers were designed using consensus sequences. For construction of yeast expression vector (pMatrix-GFP or pNida-3), matrix genes was amplified from freshly synthesized NDV cDNA. Two-step polymerase chain reaction (PCR) strategy was used for amplification of genes and installation of recombination nucleotide sequences (see Fig. 1). Recombination sequences will later be used for cloning of genes into 2-μ expression vector. In the first-step PCR using set of primers (PNida3-F/-R; Table 1), matrix gene was amplified along with incorporation of a part of recombination sequences. Complete incorporation of recombination nucleotide sequences into first-step PCR product of matrix gene was accomplished by using adapter primers (Table 1) in a second PCR. Finally, to generate expression vector (pMatrix-GFP or pNida-3), purified *Sma*I-restricted 2-μ expression vector and gel-extracted second-step PCR-amplified products of matrix gene were mixed as described before (Drew et al. 2008). Mixture was directly transformed into competent *Saccharomyces cerevisiae* cells for expression studies or for selection of recombinant vectors into *E. coli* strain OmniMax T1.

For expression of matrix gene in *E. coli*, two constructs pNida-1 and pNida-4vi were made to express the target protein in fusion with N-terminal His_6 or C-terminal maltose binding protein (MBP)-His_8 fusion, respectively. Matrix gene was amplified using two sets of primers (pNida1-F/-R or pNida4vi-F/-R; Table 1) and restriction sites *Nco*I and *Sal*I or *Stu*I and *Nco*I were incorporated at the 5′ and 3′ ends of amplified DNA to clone the fragments into respective sites of pET28a (Novagen) or pKLD116vi (Rocco et al. 2008) to generate pNida-1 or pNida4vi, respectively. All genetic manipulation was carried out in the *E. coli* strain OmniMAX™ 2T1. Initially, constructs were confirmed by colony PCR using primers corresponding to a region of T7 promoter/T7 terminator (see Table 1) and then verified by DNA sequencing. Nucleotide sequence of amplified gene was found to be identical to a sequence of matrix gene (Acct. No. GU182328.1) of a Pakistani NDV isolate, already deposited in the NCBI GenBank.

Expression of M-protein in *S. cerevisiae*

For expression of M-protein in *S. cerevisiae*, mixture containing PCR product corresponding to matrix gene and *Sma*I-linearized 2-μ vector or expression construct pMatrix-GFP

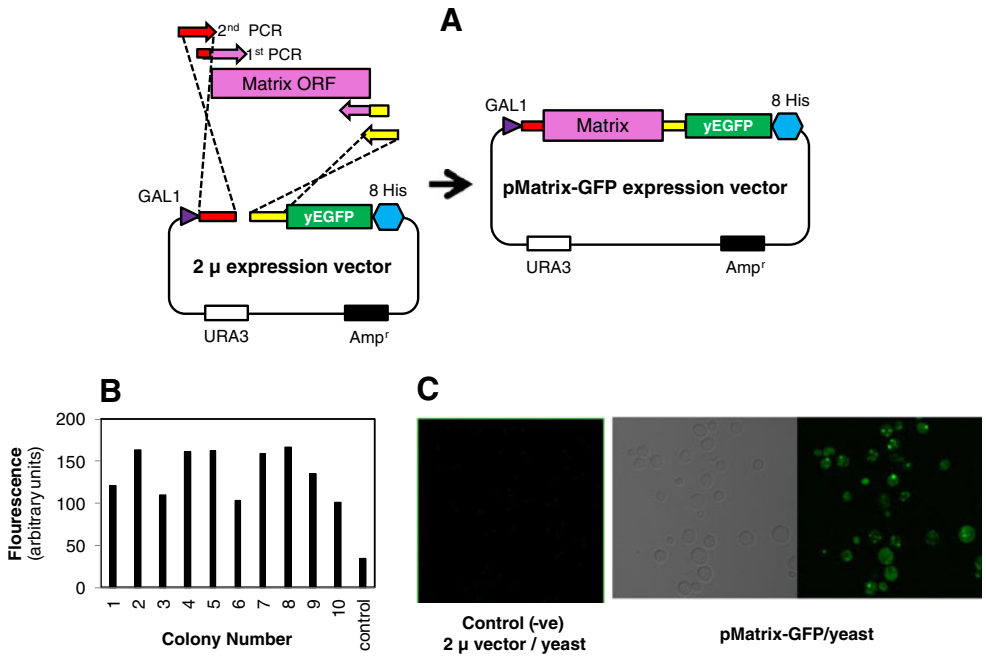

Fig. 1 Expression of M-protein in *S. cerevisiae*. **a** Strategy for recombinational cloning of the matrix gene into yeast expression vector. Amplification of the matrix gene and incorporation of recombination sites for cloning by two-step PCR was performed as described in "Materials and methods." The matrix gene containing recombination sites (installed by PCR and shown in *red* and *yellow* in primers) was mixed with *Sma*I-restricted 2-µ expression vector (carrying same recombination nucleotide sequence as that installed in genes by PCR and shown in *red* and *yellow thick lines*) to generate the expression vector pMatrix-GFP. Various elements of the 2-µ vector such as *Gal*I promoter and genes for selection markers URA3 (uracil) and Amp^r are shown. **b** Expression analysis of the matrix-GFP fusion followed by measuring whole cell fluorescence of yeast cells harboring pMatrix-GFP vector (1–10) and vector only control (2-µ expression vector). **c** Expression of matrix-GFP confirmed in the yeast cells by confocal microscopy

were transformed in uracil-deficient (URA) strain of yeast FGY217. Transformants were selected on URA media (0.2 % yeast synthetic drop-out medium, 0.67 % yeast nitrogen base without amino acids, and 2 % glucose). A number of colonies of yeast transformants containing pMatrix-GFP or 2-µ vector were inoculated in 10 mL URA medium in a 50-mL falcon tube and were grown at 30 °C in an orbital shaker at 280 rpm for 16 h; 10 µL of each overnight culture was spotted onto a fresh URA plate, allowed to dry at RT, and transferred to 30 °C incubator for 1–2 days. Then the rest of the overnight culture was diluted to an OD_{600} of 0.12 into 50 mL tubes, each containing 10 mL URA medium with 0.1 % glucose and grown in an orbital shaker at 280 rpm at 30 °C until the OD_{600} reached to 0.6. Expression of matrix-GFP F-protein was induced by adding 20 % galactose (final 2 %). After 22 h of induction, the OD600 was measured and cells were harvested at 3,000×*g* for 5 min for analysis.

Table 1 Oligonucleotides used in this study

Name	Sequence
pNida1-F	5′-CATG ccatgg TGGACTCATCTAGGACA ATTG-3, *Nco*I
pNida1-R	5′-ACGC gtcgac TTTCTTAAAAGGATTGT ATTTG-3, *Sal*I
pNida4vi-F	5′-CCA aggcct GATGGACTCATCTAGGA CAATTG-3′ *Stu*I
pNida4vi-R	5′-CATG ccatgg TTATTTCTTAAAAGGA TT-3, *Nco*I
T7 promoter	5′-TAATACGACTCACTATAGGG-3′
T7 terminator	5′-GCTAGTTATTGCTCAGCG-3′
pNida3-F	5′-TAGTGGATCCCCCATGGACTCATCT AGGACAATTG-3′
pNida3-R	5′-ATAAATTTTCCCCTTTCTTAAAA GGATTGTATTTG-3′
Adapter-F	5′-TCGACGGATTCTAGAACTA GTGGATCCCCC-3′
Adapter-R	5′-AAATTGACCTTGAAAATAT AAATTTTCCCC-3′

Nucleotides representing respective restriction sites are underlined

Expression analysis by confocal microscopy

The yeast cells from above expression experiment were resuspended in 1 mL of URA medium containing 50 % glycerol. Glycerol slows yeast mobility to facilitate the capture of quality images of GFP fluorescence. For expression analysis and to probe localization of M-protein in subcellular parts of *S. cerevisiae* cells, 1 µL of cell suspension was put on a glass slide and fluorescence of GFP fused to M-protein was measured using the confocal microscope at NIBGE and University of Liverpool, UK.

Expression of M-protein in *E .coli*

For expression in *E. coli*, recombinant plasmid constructs (pNida-1or pNida-4vi) and vector only controls (pET28a or pKLD116vi) were transformed into *E. coli* strain Rosetta 2(DE3) (Novagen). A bunch of transformed colonies corresponding to pET28a or pKLD116vi based expression constructs were picked from Luria Britani (LB) agar plates containing 40 μg/mL kanamycin and 25 μg/mL chloramphenicol or 100 μg/mL ampicillin and 25 μg/mL chloramphanicol, respectively and transferred into 10–20 mL of LB media containing appropriate antibiotics. Cultures were grown overnight at 37 °C, 220 rpm and next day diluted 100 times with expression LB media supplemented with appropriate antibiotics. Diluted cultures were then grown to an OD_{600} of ~0.4. Before induction of protein expression cultures were kept at 4 °C for ~20 min and then induced with 0.25 mM or indicated concentration of isopropyl β-D-thiogalactoside (IPTG) and were grown for further 5 h at 22 °C, 220 rpm. The cells were harvested by centrifugation at 4000×*g* at 4 °C for 20–30 min. Expression of proteins was analyzed by SDS-PAGE.

Refolding and purification of M-protein

E. coli cells containing over-expressed matrix-MBP protein were resuspended in 50 mM Tris–HCl, pH 7.9 (1 g wet biomass/8 mL buffer) and disrupted by Cell disruptor (Constant Systems®, UK) at pressure, 20 kpsi. Cell lysate was spun at 12,000×*g*, 4 °C for 30 min to harvest inclusion bodies (IBs). IBs were washed twice with 50 mM Tris–HCl at pH 7.9 and collected by centrifugation. IBs were then solubilized in denaturing buffer (Tris–HCl at pH 7.5 containing 1 mM EDTA and 8 M urea; 12.5 mg inclusion bodies/mL buffer) with help of pestle and mortar. This mixture was then passed through a narrow needle several times to ensure maximum solubilization of IBs. Mixture was then centrifuged at 14,000×*g* for 20 min to separate solubilized fraction from insoluble components.

Refolding process of M-protein was initiated by drop wise addition of refolding buffer (20 mM Tris–HCl at pH 7.9 buffer containing 1 mM NaCl and 5 % (*v*/*v*) LDAO) into solubilized IBs in 1:1 ratio while stirring vigorously at room temperature as described earlier (Saleem et al. 2012). Mixture was kept stirring at room temperature for further an hour and then dialyzed against 50 mM Tris–HCl, pH 7.9 containing 0.5 M NaCl until concentration of urea reach well below 10 mM. Any insoluble material was removed by centrifugation at 14,000×*g*, and supernatant was passed twice through Ni-nitrilotriacetate agarose equilibrated with washing buffer (20 mM Tris–HCl buffer at pH 7.9 containing 0.5 M NaCl, 30 mM imidazole, 2 mM beta mercaptoethanol, and 0.04 % (*v*/*v*) LDAO). The resin was washed with 40 CV wash buffer and the His_8-tagged protein was eluted using the same wash buffer except for the presence of 250 mM imidazole. Similarly, His_8-tagged MBP was purified using Ni-NTA chromatography from the soluble fraction of cell lysate. Identity of the protein was confirmed by mass spectrometry.

For immunization studies, from hazardous point of view, the mostly widely used detergent is Tween 20. Thus, for detergent exchange, M-protein bound to Ni-NTA was washed with Tween buffer (20 mM Tris–HCl, pH 7.9 containing 0.5 M NaCl, 2 mM β-mercaptoethanol and 0.05 % (*v*/*v*) Tween 20) before elution with the same Tween buffer except the presence of 250 mM imidazole. Finally, purified protein was exchanged to 10 mM PBS buffer at pH 7.4 containing 0.05 % Tween 20 for immunogenic studies.

Negative-stain EM analysis of the purified M-protein

For negative-stain EM analysis, concentration of purified MBP-Matrix was adjusted to 10–20 μg/mL in 20 mM Tris at pH 7.5, 100 mM NaCl, and 0.04 % LDAO. Three to 4 μL of protein was then applied to glow-discharged carbon-coated copper-palladium grids and left at room temperature for 1 min. Grids were washed with double-distilled deionized water twice, followed by washing with 0.75 % uranyl formate. Finally, grids were incubated with 0.75 % uranyl formate, blotted, and dried.

Characterization by circular dichroism and infrared spectroscopy

CD measurements were carried out using AVIV Model 400 sepctroplolarimeter at 25 °C with constant nitrogen flushing. Samples (300 μL) containing the purified protein at a concentration of 0.02 mg/mL in 10 mM potassium phosphate at pH 7.4 buffer were added into a Hellma quartz cuvette of 1-mm path length and scanned between 190 and 260 nm, averaging at least ten accumulations. Similarly, sample (blank) containing only phosphate buffer was scanned. Spectra were recorded at a speed of 1 nm/15 s, sensitivity 50 mdeg, bandwidth at 1 nm, resolution at 1 nm, and response time of 15 s.

CD data were analyzed using algorithm neuronal network and software structure analysis (By Delphi, CD Spectra Deconvolution, Version 2.1; http://bioinformatic.biochemtech.uni-halle.de/cdnn/). Before estimation of secondary structure, the phosphate buffer alone spectrum was subtracted from the protein spectrum. CD ellipticity arbitrary values were converted to mean residue ellipiticity (in degrees per square centimeter per decimole) and secondary structure was estimated compared with a data set available in structure analysis software. To examine the thermal stability of the purified protein, measurements were made at 222 nm during the heating of the protein from 10 to 90 °C at a rate of 1 °C/min with aversing/response time of 15 s.

For infrared spectroscopy, protein was lyophilized to a concentration of ~1 mg/mL in PBS buffer containing 0.04 % LDAO or 0.05 % Tween 20. A small amount of sample is dried on platinum ATR platform (diamond crystal) to form a hydrated film and then spectra obtained using Bruker FT-IR spectrometer. Similarly, spectra was recorded for buffer alone and subtracted from protein spectra to eliminate bending vibration of H_2O that gives strong absorption band at 1,645 cm^{-1} in the amide I region. Decomposition of the spectra into individual bands in the amide I region was performed by nonlinear peak fitting using Galactic PeakSolve™ software (version 1.05). Band assignments for interpretation of spectra were done on the basis of previous measurements (Goormaghtigh et al. 1994a).

Immunization and challenge studies

One-day-old 60 broiler chicks were purchased from commercial hatchery (Arus Chicks, Faisalabad) which were not immunized against NDV or any other agent and kept under standard managemental conditions in an animal house. The experiment was conducted under the regulations of the Institutional Animal Care and Use Committee of Animal Sciences Division, NIAB, Faisalabad, Pakistan. These chicks were divided in 6 groups having 10 broiler chicks in each group. The purified recombinant protein was quantified by Bradford essay and adjuvanted with Freund's complete adjuvant (FCA) in 1:1 ratio. At 7th day of age, chicks in group A were injected subcutaneously, each with ~40 μg of adjuvant MBP-M-protein (Arora et al. 2010). Group B was injected subcutaneously with ~40 μg of maltose binding protein with FCA per chick. Group C was vaccinated with commercially available kill vaccine against NDV. Group D was vaccinated with commercially available live vaccine against NDV. Groups E and F were injected with sterile phosphate buffer saline (200 μL/bird) and they were treated as challenge control and negative control respectively. Group A was given subcutaneously a boaster dose of ~40 μg recombinant MBP-M-protein after 21 days of first immunization. Blood samples were collected pre-immunization and with 7-day intervals till 28th days post-immunization from birds in each group (wing vein route).

During challenge protection studies, broiler chicks of all groups (A, B, C, D, and E) were challenged with pathogenic NDV having $10^{4.7}$ EID_{50}/0.1 mL by intraocular route at 25 days post-immunization. Group F was treated as negative control as it received PBS in the same way. Chicks of all groups were kept under observation for 5 days.

For determination of antibody titer in serum against M-protein and relevant controls, purified MBP-M-protein (4 μg/well) was coated as antigen on 96-well ELISA plate and serum collected from each group pre and post immunization was added as primary antibody at various dilutions in phosphate buffer saline. Antibody titers were determined using anti-chicken IgG alkaline phosphatase conjugate (Sigma) as secondary antibody and p-nitrophenyl phosphate as substrate (MP Biomedicals).

Results

Expression of the M-protein in *S. cerevisiae*

M-proteins have been successfully expressed in eukaryotic cell lines (Harrison et al. 2010; Molouki et al. 2011; Wang et al. 2009; Yin et al. 2010). We here exploited *S. cerevisiae* as a eukaryotic model organism to express the matrix gene. To achieve this, the ORF for the M-protein was first cloned into a 2-μ yeast expression vector by recombinatorial cloning (Fig. 1a). Yeast cells over-expressing the GFP-tagged M-protein were screened by measuring the GFP-fluorescence and by confocal microscopy of small-scale cell cultures (Fig. 1b, c). Expression levels of the chimera were relatively low. Although such expression levels can prove useful to investigate the interaction between the M-protein and other NDV proteins (like NH, F, or NP) in the yeast cell during viral assembly, we could not obtain sufficient amounts of purified protein for structural and functional analysis.

Expression of the M-protein in *E. coli*

To obtain purified protein in amounts required for functional studies, we expressed the M-protein in fusion with a C-terminal His_6-tag or an N-terminal His_8-MBP in a codon optimized *E. coli* Rosetta 2 (DE3) strain. In both cases, protein expression yielded a strong band migrating at ~41 or ~83 kDa for C- or N-terminally tagged M-protein, respectively (Fig. 2a, b). However, all overexpressed protein localized in inclusion bodies (IB) (Fig. 2a). The identity of expressed 83 kDa protein was further confirmed by Western blotting using antibodies against His_8-tag (Fig. 2b). Enhancing M-protein solubility by variation of the IPTG concentration, growth temperature or the co-expression of chaperonins cpn10 and cpn60 in Arctic express® *E. coli* cells for refolding at low temperature (Stratagene) (Ferrer et al. 2003), was not successful (data not shown). We therefore pursued in vitro refolding following protein expression in inclusion bodies.

Refolding and purification of the M-protein

Refolding of Matrix-His_6 and His_8-MBP-Matrix was first initiated by solubilization of the inclusion bodies in 8 M urea and overnight dialysis in 20 mM Tris–HCl buffer, pH 7.9, containing 100 mM NaCl. Although a significant part of His_8-MBP-Matrix was solubilized following this procedure,

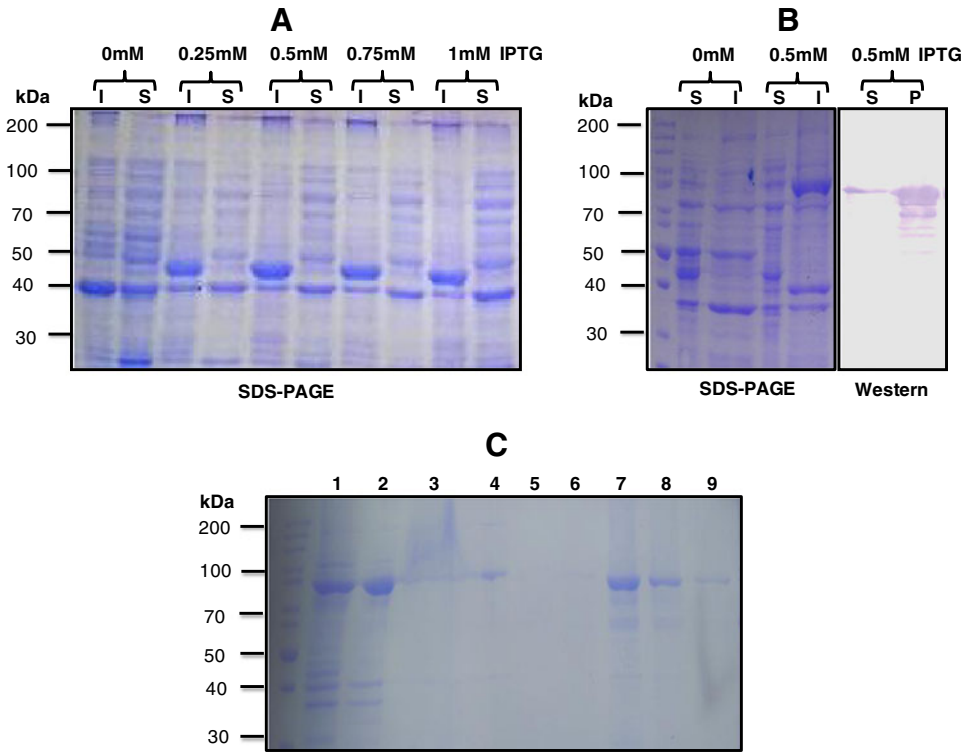

Fig. 2 Expression of Matrix-His6 (**a**) and His8-MBP-Matrix (**b**) in *E. coli* strain Rosetta 2 (DE3) and purification of refolded of His_8-MBP-Matrix by Ni-NTA affinity chromatography (**c**). *I* insoluble (inclusion body), *S* soluble fraction of lysate obtained from cultures harboring pNida1 (**a**) or pNida4vi (**b**) induced with indicated concentration of isopropyl-β-D-thiogalactoside (*IPTG*). Identity of His8-MBP-Matrix (**b**) is confirmed by Western blot analysis using antibodies against oligohistidine tag. **c** SDS-polyacryl amide gel stained with Coomassie brilliant blue, showed proteins from insoluble fraction of lysate of *E. coli* cultures contained expressed His_8-MBP-Matrix (*lane 1*), proteins solubilized in 8 M urea (*lane 2*), refolded fraction (*lane 3*), unbond fraction from Ni-NTA chromatography (*lane 5*), wash fraction (*lane 5*), and purified protein fractions eluted from Ni-NTA column (*lanes 7–9*) as described in "Material and methods." The mobilities of marker proteins of known molecular mass are shown on the *left*

the protein was unstable and precipitated (data not shown). To investigate whether the relatively high hydrophobicity of the protein sequence (predicted by hydropathy analysis; http://www.ebi.ac.uk/Tools/seqstats/emboss_pepinfo) required the presence of a detergent, refolding was attempted in the presence of the non-ionic detergent *N,N*-dimethlydodecylamine *N*-oxide (LDAO), as described in "Material and methods." LDAO-assisted refolding indeed increased protein solubility and thus refolded M-protein was subsequently purified by Nickel affinity chromatography to ~95 % purity in quantities sufficient for structural and immunogenic studies (Fig. 2c). Mass spectrometry confirmed that the purified protein was full length and trypsin digestion identified 11 peptides with 24 % overall protein coverage (Fig. 3a). Negative-stain electron microscopy analysis further indicated that the purified protein may exist in several oligomeric forms in solution, indicated by the presence of particles of different size (Fig. 3b). This is in agreement with previous reports on the biophysical analyses of the NDV M-

Fig. 3 Analysis of purified His8-MBP-Matrix by mass spectroscopy (MS) and electron microscopy (EM). **a** MS analysis identified 11 distinct peptides corresponding to M-protein shown with increasing mass order. **b** EM analysis of the purified protein in 0.04 % LDAO: *arrows* indicate particles of different sizes representing various oligomeric form of the protein

A

Amino acid Position	Mass	Sequence
360-364	668.7704	YNPFK
360-365	796.9445	YNPFKK
149-156	867.9775	YSSVNAVK
328-336	1000.1861	IIIQAGTQR
315-324	1191.4337	ILWSQTACLR
174-184	1203.4675	VNFVSLTVVPK
149-159	1232.4253	YSSVNAVKHVK
144-156	1379.5994	VVANKYSSVNAVK
337-350	1429.5702	AVAVTADHEVTSTK
337-353	1800.0192	AVAVTADHEVTSTKLEK
228-249	2502.8475	SDSGYYANLFLHIGLMTTVDRK

B

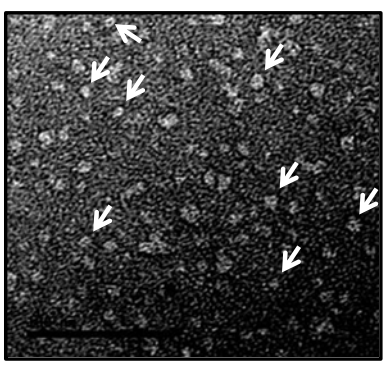

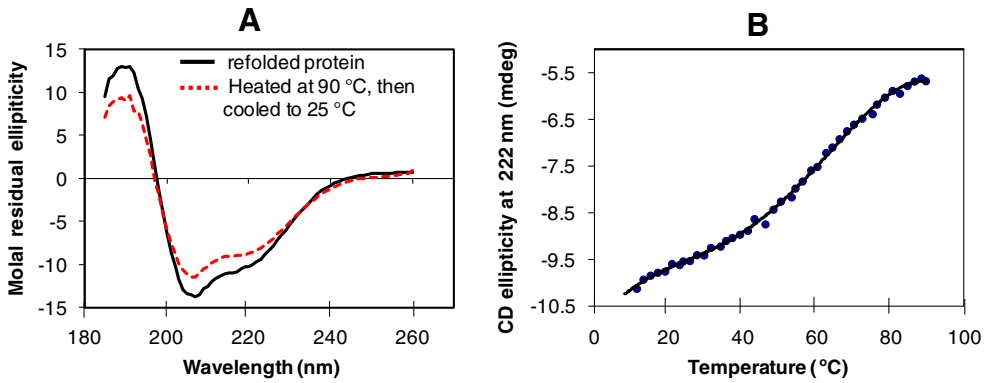

Fig. 4 Characterization of His_8-MBP-Matrix by circular dichroism spectroscopy. **a** CD spectra of refolded (*continuous line*) and thermally unfolded/refolded, i.e., heated at 90 °C followed by cooling to 25 °C (*dotted line*) of His_8-MBP-Matrix. **b** Thermal unfolding of purified His_8-MBP-Matrix. CD measurements were made during the heating of the protein at a rate of 1 °C/min

protein (Battisti et al. 2012) and of M-proteins from Borna disease virus (Kraus et al. 2005), respiratory syncytial virus (Money et al. 2009), and Ebola virus (Timmins et al. 2003; Han et al. 2003).

Structural characterization of the M-protein

Successful refolding was verified by comparing the secondary structure components obtained from CD and FT-IR spectroscopies to the crystal structures of the NDV M-protein and the structural analysis of other known M-protein homologues. Both CD and FT-IR spectra were indicative of protein consisting of mixed secondary structure components (Figs. 4 and 5). To provide quantitative estimate of the alpha-helical and beta-sheet content of the protein, hydrated films were investigated using FT-IR. The measured amide I region of the spectrum (Fig. 5a, top) could be reproduced by a fit of 11 components, dominated by those indicative of alpha-helix and beta-sheet (Arrondo et al. 1993; Goormaghtigh et al. 1994a, b) (Fig. 5b). Quantitative analysis of the spectrum predicted the presence of ~29 % alpha-helix and ~27 % beta-sheet structures, as expected from the crystal structures of MBP and the M-protein (Table 2) (Quiocho et al. 1997; Battisti et al. 2012; Kabsch and Sander 1983).

CD spectra of the protein showed minima around 208 and 220 nm and a maximum between 190 and 195 nm (Kelly et al. 2005). Secondary structure estimated by the analysis of the spectrum (Fig. 4a; continuous line) agreed well with that determined from FT-IR spectra, yielding 23 and 30 % for alpha-helix and beta-sheet components, respectively, confirmed that the protein extracted from inclusion bodies had adopted the expected secondary structure components upon

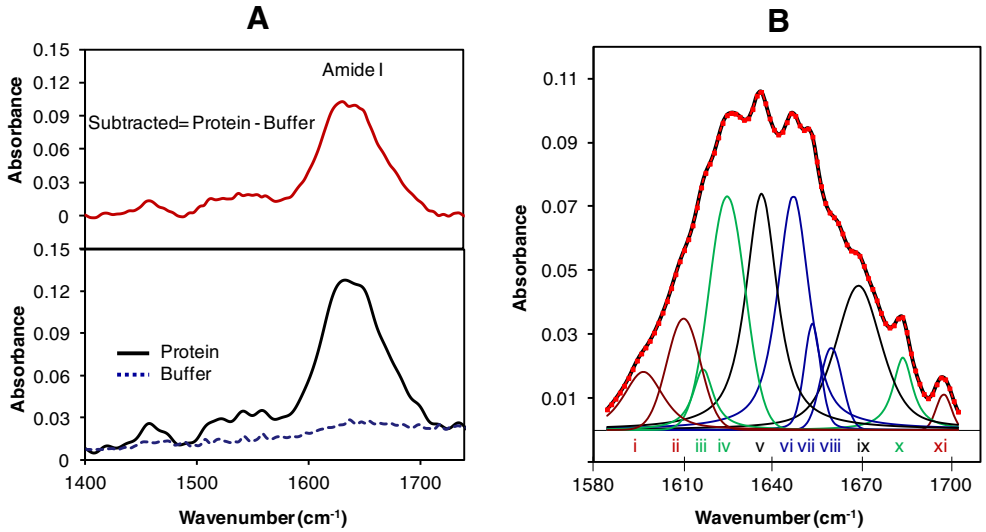

Fig. 5 Analysis of His_8-MBP-Matrix secondary structure by FT-IR. **a** *Bottom*, FT-IR spectra of hydrated film of PBS buffer and His_8-MBP-Matrix. *Top*, final protein spectrum obtained by subtraction of His_8-MBP-Matrix from buffer spectrum. **b** Amide I region of the FTIR spectrum of a hydrated film of His_8-MBP-Matrix (*thick black line*), and bands obtained by deconvolution. The latter were assigned to unordered structure (*i*, *ii*, and *xi*), beta-sheet (*iii*, *iv*, and *x*), alpha-helix (*vi*, *vii*, and *viii*), and beta-turns (*v* and *ix*). The *dotted red line* shows the curve fitted using these component bands

Table 2 Analysis of His_8-MBP-Matrix protein using FT-IR and CD spectroscopy

Methods/techniques	α-helix (%)	β-sheet (%)
FT-IR[a]	29	27
CD[b]	23	30
DSSP[c]	31.5	29

[a] Bands contributing (FT-IR spectra) to each type of secondary structure are indentified in Fig. 5b. Bands assignments for interpretation of spectra were made on the basis of previous measurements (Goormaghtigh et al. 1994a)

[b] CD spectrum was analyzed using algorithm neuronal network and structure analysis program as described in "Material and methods"

[c] Secondary structure (as per dictionary of protein secondary structure (DSSP)) of MBP-Matrix protein were obtained from X-ray structures (1ANF and 4G1G) available in PDB (Quiocho et al. 1997; Battisti et al. 2012; Kabsch and Sander 1983)

refolding. To further investigate whether the protein was refolded correctly, the structural integrity of the refolded protein was analyzed by thermal unfolding, monitoring spectral changes in CD ellipticity at 222 nm. Stepwise heat denaturation of the protein to 90 °C showed a cooperative transition during the unfolding of the M-protein indicative of a stable core and indeed suggesting that the M-protein was correctly refolded (Fig. 4b). Thermal denaturation of the M-protein was largely reversible since the CD spectrum of the protein showed similar features to the native protein upon cooling to 25 °C. The decrease in amplitude of the molar residual ellipticity after cooling the heated protein likely reflected degradation of a small amount of the protein during the course of heating/cooling.

Immunogenicity and challenge protection test

Immunogenic studies were performed in chickens as described in the materials and methods section. Serum antibody titers, determined by ELISA, revealed that a significant amount of antibodies were produced in chicken against the M-protein (group A) compared with controls (Fig. 6). Despite this, birds in group A were prone to disease as only 30 % protection was achieved and the birds were showing typical symptoms of Newcastle disease after 36–48 h of viral challenge. Signs and symptoms observed were off feed, conjunctivitis, gasping, coughing, nasal discharge and greenish, watery diarrhea. High mortalities were also observed 48–96 h post-infection in different groups (Table 3). In contrast, groups of those vaccinated with killed and live vaccines (C and D) were showing 70 and 90 % protection, respectively. Only mild/moderate signs and symptoms of the disease were observed in the birds of these groups. No symptoms of the disease were observed in the negative control group (E) while severe and typical signs of velogenic viscerotropic Newcastle disease were observed along with high mortalities in challenge control group (F). Due to high mortalities in various groups after infection, the uniform number of serum samples could not be collected to detect antibody titers at 7th-day post-infection. During postmortem examinations of dead birds, prominent signs and symptoms of the disease were observed, including an enlarged spleen and hemorrhages on proventriculus (Fig. 7). Thus, even though significant amounts of antibodies were raised within the chickens, the M-protein appeared to play least role in conferring protection (30 %) against pathogenic NDV (Table 3).

Discussion

We here reported on the heterologous expression of the NDV M-protein in *S. cerevisiae* and *E. coli* for the characterization of its role in virus assembly and budding and to explore its potential for the development of new antivirals. The M-protein is located within the virus particle, however, we reasoned that it would be a potent antivirus target because of its many roles in the virus life cycle and its high degree of conservation (Farsang et al. 2003; Khan et al. 2010; Zanetti et al. 2003; Seal et al. 2000).

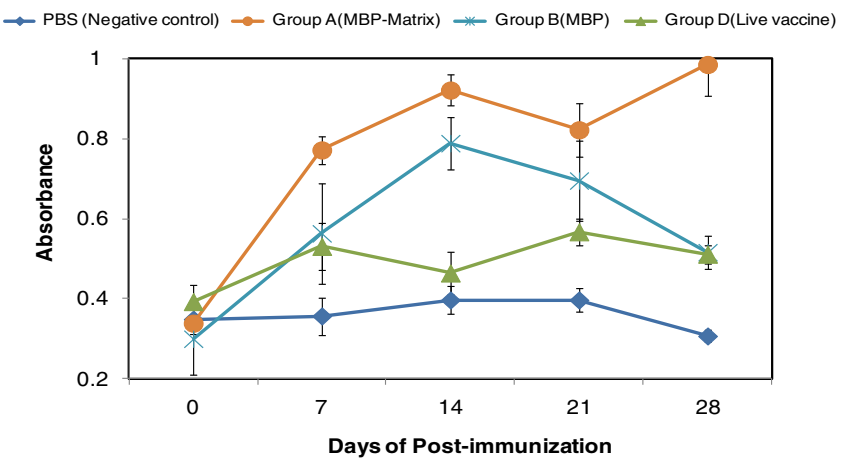

Fig. 6 Antibody titers in treatment and control groups after immunization. After 21 days of first immunization, a booster dose was given to chickens in group A

Table 3 Morbidity and mortality data of broiler chicken in immunization studies

Group	Treatment at 7th day	Protein/vaccine	Challenge	Morbidity	Mortality	Lesions score	Survived	Protection (%)
A	Treated	MBP-Matrix protein	25th day	9/10	7	+++	3/10	30
B	Treated	Maltose binding protein	25th day	10/10	8	++++	2/10	20
C	Treated	Killed vaccine	25th day	4/10	3	++	7/10	70
D	Treated	Live vaccine	25th day	2/10	1	+	9/10	90
E	Control	Sterile PBS (negative control)	Sterile PBS	0/10	0	−	10/10	100
F	Control	Sterile PBS (challenge control)	25th day	10/10	9	++++	1/10	10

Lesion score: "++++" severe, "+++" moderate, "++" mild, "+" minute, "–" no lesions

The NDV M-protein was expressed in inclusion bodies in our hands. Subsequent refolding yielded a protein with similar secondary structure to the known NDV M-protein structure (Battisti et al. 2012). In a recent study, Money et al. (2009) compared structural features of M-protein of respiratory syncytial virus (RSV) present in its crystal structure with that of obtained by CD spectroscopy in solution. Their data indicate that secondary structure content of RSV matrix in solution is significantly lower than that observed in the crystalline state, particularly in case of β-sheet. Evaluation of CD and X-ray crystallographic data give 23 and 47 % β-sheet contents, respectively. On the basis of this, they have suggested that assembly of M-protein is associated with significantly unfavorable entropic contribution from protein folding which is in common with the binding of disordered proteins to their counterparts. In case of RSV matrix, such interactions may be achieved in the protein itself, with NP, the viral glycoprotein HN and F, via their cytolplasmic tails and with the host cell and viral membrane which are thought to be essential for the assembly and budding of a virion particle and could contribute to stabilizing the structure (Money et al. 2009). On the other hand, no such large difference in secondary structure composition of NDV matrix were observed, determined in solution by CD and FT-IR (Table 2), and obtained from crystal structure (Battisti et al. 2012). This might be due to reason that the crystal structure of NDV M-protein is a dimer whereas RSV matrix is monomer; hence stabilized by multiple interactions between monomers. Moreover, RSV matrix is crystallized in truncated form, missing 25 C-terminal residues, including those that comprise α-helix 13 in NDV which is involved in the monomer-to-monomer contact within the dimer (Battisti et al. 2012).

Consistent with the reports of others (Kraus et al. 2005; Money et al. 2009; Han et al. 2003; Timmins et al. 2003), the refolded M-protein oligomerized in solution. Significant antibody serum titers were obtained in chickens upon immunization with recombinant M-protein, however, the antibodies failed to give protection against lethal viral challenge and infected chickens exhibited typical symptoms of the Newcastle disease 48–96 h post-infection. We conclude therefore that the NDV M-protein (or the part against which the antibodies were raised) may not be exposed on the surface of the NDV or the host cell at any stage of virus assembly and budding. In contrast to NDV M-protein, mice and rabbit immunized with M-protein 2 of influenza virus show significant protection against lethal influenza virus challenge (Ebrahimi and Tebianian 2010; El Bakkouri et al. 2011). This might be due to the reason that a part of influenza virus M-protein 2 is located on the surface of virus compared to NDV M-protein that is present inside the virion. Nonetheless, the M-protein may still be a valuable target for antiviral drug compounds. Indeed, the M-protein appears to have many roles in virus maturation and interacts with many of the other viral proteins (HN, F, and N), as well as with host proteins. Increased understanding of these interactions, for example, by co-crystallization of M with its partners, will facilitate the design of new drug compounds.

Previously, the interactions between M-proteins and its partners of other paramyxovirusses have been characterized in eukaryotic cell lines (Ali and Nayak 2000; Waning et al. 2002; Schmitt et al. 2010; Chen et al. 2008). The successful expression of the M-protein in yeast and its targeting to the yeast membrane obtained here are promising to further develop

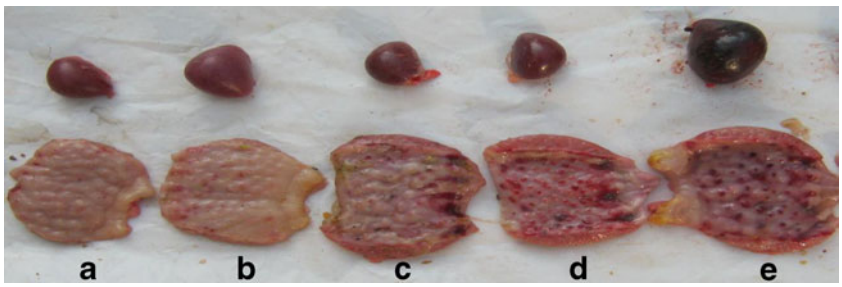

Fig. 7 Spleen and proventriculus showing varying degree of postmortem lesions (enlarged spleen and hemorrhages on proventriculus). *a* No lesions, *b* minute lesions, *c* mild lesions, *d* moderate lesions, and *e* severe lesions

interaction assays for M-proteins and its partners (like HN, F, and NP) in a versatile host that is also easily manipulated.

Together, the expression of the M-protein in yeast and *E. coli* provides a platform for a multidisciplinary approach to elucidate the interactions and the structures of the M-protein with its partners. The detailed insights obtained from such combined analyses will facilitate rational design of new virus inhibitors needed in the poultry industry.

Acknowledgments We thank S.A Baldwin, University of Leeds, UK, for provision of yeast construct/strain; J. C. Escalante-Semerena, University of Wisconsin, USA, for MBP-*E. coli* expression vector; F. Nurjis and S. Hameed at NIBGE, and Awais at University of Liverpool, UK, for confocal microscopy studies; O, Gursky, Boston University, USA, for assistance with CD spectroscopy analysis, S. Ashraf and I. Hussain, LUMS University, Pakistan, for recording IR spectra. We grateful to G.H.M. Huysmans, Pasteur Institute, France, for comments and manuscript's improvement. This work was supported by the Higher Education Commission of Pakistan (grant No. 20-2138 (awarded to M. Rahman) and Ph.D. studentship (awarded to N. Iram)) and International Atomic Energy Agency (Fellowship awarded to M. Rahman). The authors declare that they have no conflict of interest.

References

Ali A, Nayak DP (2000) Assembly of Sendai virus: M protein interacts with F and HN proteins and with the cytoplasmic tail and transmembrane domain of F protein. Virology 276:289–303

Arora P, Lakhchaura BD, Garg SK (2010) Evaluation of immunogenic potential of 75 kDa and 56 kDa proteins of Newcastle disease virus (NDV). Indian J Exp Biol 48:889–895

Arrondo JL, Muga A, Castresana J, Goni FM (1993) Quantitative studies of the structure of proteins in solution by Fourier-transform infrared spectroscopy. Prog Biophys Mol Biol 59:23–56

Battisti AJ, Meng G, Winkler DC, McGinnes LW, Plevka P, Steven AC, Morrison TG, Rossmann MG (2012) Structure and assembly of a paramyxovirus matrix protein. Proc Natl Acad Sci U S A 109:13996–14000

Chambers P, Millar NS, Bingham RW, Emmerson PT (1986) Molecular cloning of complementary DNA to Newcastle disease virus, and nucleotide sequence analysis of the junction between the genes encoding the hemagglutinin neuraminidase and the large protein. J Gen Virol 67:475–486

Chen J, Zhou J, Bae W, Sanders CK, Nolan JP, Cai H (2008) A yEGFP-based reporter system for high-throughput yeast two-hybrid assay by flow cytometry. Cytom A 73A:312–320

Chomczynski P, Sacchi N (1987) Single-step method of RNA isolation by acid guanidinium thiocyanate phenol chloroform extraction. Anal Biochem 162:156–159

Drew D, Newstead S, Sonoda Y, Kim H, von Heijne G, Iwata S (2008) GFP-based optimization scheme for the overexpression and purification of eukaryotic membrane proteins in *Saccharomyces cerevisiae*. Nat Protoc 3:784–798

Adu-Gyamfi E, Soni SP, Xue Y, Digman MA, Gratton E, Stahelin RV (2013) The Ebola virus matrix protein penetrates into the plasma membrane: a key step in viral protein 40 (VP40) oligomerization and viral egress. J Biol Chem 288:5779–5789

Ebrahimi SM, Tebianian M (2010) Heterologous expression, purification and characterization of the influenza A virus *M2e* gene fused to *Mycobacterium tuberculosis* HSP70 (359–610) in prokaryotic system as a fusion protein. Mol Biol Rep 37:2877–2883

El Bakkouri K, Descamps F, De Filette M, Smet A, Festjens E, Birkett A, Van Rooijen N, Verbeek S, Fiers W, Saelens X (2011) Universal vaccine based on ectodomain of matrix protein 2 of influenza A: Fc receptors and alveolar macrophages mediate protection. J Immunol 186:1022–1031

Farsang A, Wehmann E, Soos T, Lomniczi B (2003) Positive identification of Newcastle disease virus vaccine strains and detection of contamination in vaccine batches by restriction site analysis of the matrix protein gene. J Vet Med B Infect Dis Vet Public Health 50:311–315

Ferrer M, Chernikova TN, Yakimov MM, Golyshin PN, Timmis KN (2003) Chaperonins govern growth of *Escherichia coli* at low temperatures. Nat Biotechnol 21:1266

Goormaghtigh E, Cabiaux V, Ruysschaert JM (1994a) Determination of soluble and membrane protein structure by Fourier transform infrared spectroscopy. I. Assignments and model compounds. Subcell Biochem 23:329–362

Goormaghtigh E, Cabiaux V, Ruysschaert JM (1994b) Determination of soluble and membrane protein structure by Fourier transform infrared spectroscopy. III. Secondary structures. Subcell Biochem 23:405–450

Grimes SE (2002) A Basic Laboratory Manual for the Small Scale Production and Testing of I-2 Newcastle Disease Vaccine. Food and Agricultural Organization (FAO), Animal Production and Health Commission for Asia and the Pacific (APHCA)

Han ZY, Boshra H, Sunyer JO, Zwiers SH, Paragas J, Harty RN (2003) Biochemical and functional characterization of the Ebola virus VP24 protein: implications for a role in virus assembly and budding. J Virol 77:1793–1800

Harrison MS, Sakaguchi T, Schmitt AP (2010) Paramyxovirus assembly and budding: building particles that transmit infections. Int J Biochem Cell Biol 42:1416–1429

Hierholz JC, Suggs MT, Hall EC (1969) Standardized viral hemagglutination and hemagglutination-inhibition tests .2. Description and statistical evaluation. Appl Microbiol 18:824–833

Hoenen T, Biedenkopf N, Zielecki F, Jung S, Groseth A, Feldmann H, Becker S (2010) Oligomerization of Ebola virus VP40 is essential for particle morphogenesis and regulation of viral transcription. J Virol 84:7053–7063

Kabsch W, Sander C (1983) Dictionary of protein secondary structure—pattern-recognition of hydrogen-bonded and geometrical features. Biopolymers 22:2577–2637

Kelly SM, Jess TJ, Price NC (2005) How to study proteins by circular dichroism. Biochim Biophys Acta 1751:119–139

Khan TA, Rue CA, Rehmani SF, Ahmed A, Wasilenko JL, Miller PJ, Afonso CL (2010) Phylogenetic and biological characterization of Newcastle disease virus isolates from Pakistan. J Clin Microbiol 48:1892–1894

Kraus I, Bogner E, Lilie H, Eickmann M, Garten W (2005) Oligomerization and assembly of the matrix protein of Borna disease virus. FEBS Lett 579:2686–2692

Molouki A, Hsu YT, Jahanshiri F, Abdullah S, Rosli R, Yusoff K (2011) The matrix (M) protein of Newcastle disease virus binds to human Bax through its BH3 domain. Virol J 8:385

Money VA, Mcphee HK, Mosely JA, Sanderson JM, Yeo RP (2009) Surface features of a Mononegavirales matrix protein indicate sites of membrane interaction. Proc Natl Acad Sci U S A 106:4441–4446

Panshin A, Shihmanter E, Weisman Y, Orvell C, Lipkind M (1997) Antigenic epitope characterization of matrix protein of Newcastle disease virus using monoclonal antibody approach: contrasting variability amongst NDV strains. Comp Immunol Microbiol Infect Dis 20:177–189

Pantua HD, McGinnes LW, Peeples ME, Morrison TG (2006) Requirements for the assembly and release of Newcastle disease virus-like particles. J Virol 80:11062–11073

Peeples ME, Bratt MA (1984) Mutation in the matrix protein of Newcastle-disease virus can result in decreased fusion glycoprotein incorporation into particles and decreased Infectivity. J Virol 51:81–90

Peeples ME, Can W, Gupta KC, Coleman N (1992) Nuclear entry and nucleolar localization of the Newcastle-disease virus (NDV) matrix protein occur early in infection and do not require other NDV Proteins. J Virol 66:3263–3269

Quiocho FA, Spurlino JC, Rodseth LE (1997) Extensive features of tight oligosaccharide binding revealed in high-resolution structures of the maltodextrin transport chemosensory receptor. Structure 5:997–1015

Rocco CJ, Dennison KL, Klenchin VA, Rayment I, Escalante-Semerena JC (2008) Construction and use of new cloning vectors for the rapid isolation of recombinant proteins from *Escherichia coli*. Plasmid 59:231–237

Saleem M, Moore J, Derrick JP (2012) Expression, purification, and crystallization of neisserial outer membrane proteins. Methods Mol Biol 799:91–106

Schmitt PT, Ray G, Schmitt AP (2010) The C-terminal end of *Parainfluenza* virus 5 NP protein is important for virus-like particle production and M-NP protein interaction. J Virol 84:12810–12823

Seal BS, King DJ, Meinersmann RJ (2000) Molecular evolution of the Newcastle disease virus matrix protein gene and phylogenetic relationships among the paramyxoviridae. Virus Res 66:1–11

Timmins J, Schoehn G, Kohlhaas C, Klenk HD, Ruigrok RWH, Weissenhorn W (2003) Oligomerization and polymerization of the filovirus matrix protein VP40. Virology 312:359–368

Wang L, Suo X, Chen FY, Zheng SJ (2009) Expression of Newcastle disease virus (NDV) M protein from a recombinant plasmid prolongs the survival of NDV-infected chicken embryos and enhances the virus replication. Acta Virol 53:105–110

Waning DL, Schmitt AP, Leser GP, Lamb RA (2002) Roles for the cytoplasmic tails of the fusion and hemagglutinin-neuraminidase proteins in budding of the paramyxovirus simian virus 5. J Virol 76:9284–9297

Yin RF, Ding ZA, Liu XX, Mu LZ, Cong YL, Stoeger T (2010) Inhibition of Newcastle disease virus replication by RNA interference targeting the matrix protein gene in chicken embryo fibroblasts. J Virol Methods 167:107–111

Yusoff K, Tan WS (2001) Newcastle disease virus: macromolecules and opportunities. Avian Pathol 30:439–455

Zanetti F, Rodriguez M, King DJ, Capua I, Carrillo E, Seal BS, Berinstein A (2003) Matrix protein gene sequence analysis of avian paramyxovirus 1 isolates obtained from pigeons. Virus Genes 26:199–206

Zhang K, Wang Z, Liu XL, Yin CC, Basit ZS, Xia B, Liu WJ (2012) Dissection of influenza A virus M1 protein: pH-dependent oligomerization of N-terminal domain and dimerization of c-terminal domain. PLoS One 7:e377786